

# Effects of Copper Exchange Levels on Complexation of Ammonia in Cu (II)-exchanged X Zeolite

Chrispin O. Kowenje<sup>a,\*</sup>, David C. Doetschman<sup>b</sup>, Jürgen Schulte<sup>b</sup>, Charles W. Kanyi<sup>b</sup>, Jared DeCoste<sup>b</sup>, Szu-Wei Yang<sup>b</sup> and Barry R. Jones<sup>b</sup>

<sup>a</sup>Department of Chemistry, Maseno University, Box 333 – 40105, Maseno, Kenya.

<sup>b</sup>Department of Chemistry, Binghamton University, Vestal Parkways East, Binghamton, NY 13902-6000, USA.

Received 14 January 2009, revised 17 October 2009, accepted 23 November 2009.

## ABSTRACT

Copper (II)-exchanged faujasite-X zeolites at various loadings of copper per unit cell of zeolites were prepared and then exposed to ammonia. The copper ammine complexes of the various copper levels per unit cell were characterized and analyzed by a combination of diffuse reflectance, X-ray powder diffraction, FT-infrared spectroscopy, electron paramagnetic resonance and nuclear magnetic resonance spectroscopic methods. At low copper exchange levels (<5 copper atoms per unit cell), the major complex is  $[\text{Cu}(\text{O}_{\text{zeo}})_2(\text{NH}_3)_2]^{2+}$  and it is strongly bound to the zeolite framework walls at single four ring sites (site III). Above five copper atoms per unit cell, the major complex becomes  $[\text{Cu}(\text{NH}_3)_4]^{2+}$  and it is least interacting with the zeolite framework walls. The  $[\text{Cu}(\text{NH}_3)_4]^{2+}$  complex which was formed at higher copper levels per unit cell was most favoured by the presence of maximal amount of ammonia.

## KEYWORDS

Cation exchange, catalysis, copper, complexation, copper amines.

## 1. Introduction

Copper-exchanged zeolites are effective catalysts in decomposition of  $\text{NO}_x$ ,<sup>1</sup> conversion of hydrocarbons<sup>2</sup> and removal of sulphur components from petroleum products.<sup>3</sup> Such enhanced catalytic abilities for the cation-exchanged zeolites depend, among other factors, on the loading levels and the siting of the exchanged cations in zeolite.<sup>1</sup> In addition, the catalytic activities of cation-exchanged zeolites depend on the nature of the complexed cation centre.<sup>4</sup> The most extensively studied zeolite is faujasite-X (FAU-X). Such extensive studies are based, in part, on the extensive use of FAU-X as a support for catalysts and more recently due to increased computer-modelled FAU-adsorbate interactions.<sup>1-3,5</sup> Faujasite type zeolites possess spherical cavities (supercages) of *ca.* 11.8 Å in diameter and incorporate several cation attachment sites numbered I-III.<sup>6</sup> The faujasite framework is also associated with ring structures such as single four rings (S4R), single six rings (S6R) and double six rings (D6R).<sup>6</sup>

Among the most frequently used molecular probes in the characterization of cation-exchanged zeolites is ammonia.<sup>7</sup> Ammonia is small enough (*ca.*  $3.70 \times 3.99 \times 3.11$  Å in dimensions) that it can fit in the supercage of the faujasite and in any other cavity with  $\geq 4$  Å opening.<sup>7</sup> Due to the presence of large void volumes in the zeolite matrix, it then becomes possible for a metal complex of a strong ligand and of appropriate dimensions to form in the supercage of the zeolite. The resulting complex could have a cation centre not chemically attached to the zeolite framework oxygen ( $\text{O}_{\text{zeo}}$ ) in a manner similar to a 'ship-in-a-bottle' synthesis. Such an  $\text{O}_{\text{zeo}}$  detachment would be a preserve for adsorbates with stronger ligating strength than the framework oxygen of the zeolite. The literature is replete with reports of ammonia forming several complexes such as  $[\text{Cu}(\text{NH}_3)_4]^{2+}$  or  $[\text{Cu}(\text{NH}_3)_4(\text{O}_{\text{zeo}})_2]^{2+}$  in the X- and Y-faujasites.<sup>4,8</sup> It has been reported that ammonia is able to de-link the  $\text{Cu}^{2+}$  cation from the influence of more siliceous zeolites such as ZSM-5 and even faujasite-Y with  $\text{Si}/\text{Al} > 3$ .<sup>8</sup> However, it is not known whether

ammonia is able to de-link  $\text{Cu}^{2+}$  ions away from the influence of a cation-exchanged FAU-X ( $\text{Si}/\text{Al} = 1.23$ )  $\text{O}_{\text{zeo}}$ , especially as a function of Cu (II) exchange levels. Because of its low  $\text{Si}/\text{Al}$  ratio<sup>9</sup>, a high number of cation exchange sites and frequent usage in catalysis<sup>10</sup> and in other decontamination exercises,<sup>1</sup> FAU-X becomes a suitable medium for the spectroscopic characterization of sequential metal-ligand complexation reactions. In addition, renewed interest in the chemistry of FAU-X, especially in zeolite-adsorbate interactions by computer modelling studies,<sup>5</sup> demand a thorough complementary spectroscopic characterization of the system.

This work investigates the interactions between varying amounts of  $\text{Cu}^{2+}$  ions in combination with similarly varied amounts of  $\text{NH}_3$  per  $\text{Cu}^{2+}$  per unit cell of the zeolite. In addition this work presents, for the first time, a combination of techniques: diffuse reflectance spectroscopy (DRS), X-ray diffraction (XRD), nuclear magnetic resonance (NMR), FT-infrared (FT-IR) and electron paramagnetic resonance (EPR), with the intention completely to elucidate the siting-coordination of copper-ammonia interactions in the zeolite matrix. The combined EPR, DRS and NMR techniques were chosen to eliminate interferences from non-exchanged  $\text{Na}^+$  ions in the systems. By using varied amounts of both Cu/UC and ammonia, we intended to focus on the effect of exchange levels of Cu/UC on the complexation of  $\text{Cu}^{2+}$  in faujasite-X (CuX). To the best of our knowledge, no work has reported such an elaborate and complete analysis of the CuX-ammonia system. These findings would help maximize the tunable properties of and offer more insight into the performances of ammonia-ligated CuX as used in computer modelling and catalysis, and as sensor support materials.

## 2. Experimental

### 2.1. Materials and Sample Preparation Methods

Faujasite-X zeolite (NaX) ( $\text{Si}/\text{Al} = 1.23$ , *ca.*  $2 \mu\text{m}$  particle size, from Aldrich Chemical Company, St Louis, MO, USA), ammonium hydroxide (assay 29+ %, from Fischer Chemical Company, Pitts-

\* To whom correspondence should be addressed. E-mail: ckowenje@maseno.ac.ke

burgh, PA, USA), and copper nitrate hydrate ( $\text{Cu}(\text{NO}_3)_2 \cdot 5/2\text{H}_2\text{O}$ ) (101.7 % by EDTA complexation, from J.T. Baker Chemical Company, Phillipsburg, NJ, USA) were used. The copper (II) exchange process followed the procedure of Kowenje *et al.*<sup>11</sup> Henceforth, the determined exchange levels such as for 10 Cu(II) per unit cell of zeolite will be referred to as 10 Cu/UC. In addition, the range  $\leq 5$  Cu/UC is considered as low, between 5 and 10 Cu/UC as moderate, and  $\geq 10$  Cu/UC as high copper-exchanged (CuX) samples. A predetermined amount of CuX was consequently placed in a sample tube which was connected to an adsorbate transfer tube containing the ammonia. After successful freeze-pump-thawing of the adsorbate in the transfer tube, the interconnecting valve to the sample tube was then opened and the adsorbate allowed to vaporize over to the sample. To achieve further homogeneity, the ammonia-exposed sample was then maintained at room temperature for *ca.* 8 h, followed by warming it in a 60 °C water bath for *ca.* 30 min.

## 2.2. Spectroscopic Measurements

The X-ray diffraction data were collected at room temperature on a Scintag XDS 2000 powder diffractometer (Houghton, MI, USA), using  $\text{Cu K}_\alpha$  radiation of  $\lambda = 1.5418 \text{ \AA}$  with a solid state detector. The instrument settings were 40 kV, 30 mA, step size  $0.02^\circ (2\theta)$  and a scan rate of  $2.0^\circ \text{ min}^{-1}$ . The XRD patterns were recorded in the range  $5^\circ \leq 2\theta \leq 45^\circ$ . For the NMR measurements, the 59.6 MHz solid-state  $^{29}\text{Si}$  NMR spectra were obtained at a 4 kHz MAS spinning rate on a Bruker AC 300 NMR spectrometer (Fitchburg, MA, USA) at 7.05 T. Powder samples were packed in 7 mm zirconia rotors and run under proton decoupling conditions in a 7 mm Doty MAS probe. The chemical shifts were referenced to TMS as the external standard. A total of 512 scans, averaged for each spectrum with a  $5.0 \mu\text{s } 90^\circ$  pulse at a repetition rate of 10 s, were taken. The data were then processed with 10 Hz exponential line broadening prior to Fourier transformation.

Adequate amounts of the sample were then packed in sealed quartz glass sample cuvettes and the diffuse reflectance spectroscopy measurements obtained from 200 to 1100 nm at a resolution of 2 nm using a Perkin-Elmer Lambda 2S UV-vis spectrometer (Midland, ON, Canada) at room temperature. For FT-IR measurements, for which a Bruker Equinox 55 spectrometer (Madison, WI, USA) was used, *ca.* 0.10 g of the ground KBr-sample mixture was pressed at 10 tonne pressure for *ca.*

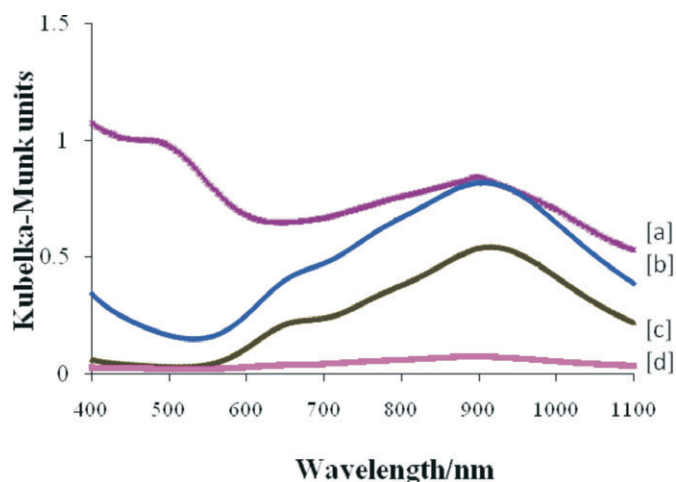


**Figure 1** DRS of CuX at different concentration levels of Cu/UC: (a) 38 Cu/UC, (b) 24 Cu/UC, (c) 10 Cu/UC, (d) 1 Cu/UC.

10 min, after which the spectrum was recorded over the  $4000\text{--}400 \text{ cm}^{-1}$  range. A total of 128 scans was collected for each sample spectrum. The continuous wave EPR (CW-EPR) spectra were recorded on an ESP E580 Bruker spectrometer (Rheinstatten, Germany) operating in the X-band ( $\sim 9.5 \text{ GHz}$ ). A field sweep from 2500–3500 G at a resolution of 1024 points in the X-axis and a modulation frequency of 100 kHz were used. Experimental EPR spectra were then fitted for the spin Hamiltonian parameters by adjustment of the hyperfine coupling constant ( $A$ ) and the electron  $g$ -value tensors with Bruker WINEPR Simfonia version 1.2, 1995.

## 3. Results

### 3.1. DRS Spectra of Different CuX Before and After Ammonia Addition

From Fig. 1, the absorption around 908 nm became more intense with increase in the concentration of the  $\text{Cu}^{2+}$  exchanged up to *ca.* 24 Cu/UC. A further increase in the amount of copper exchanged to 38 Cu/UC did not increase the intensity of the 908 nm peak, but caused a new band to appear at *ca.* 500 nm.

### 3.2. X-ray Study of CuX Exposed to Ammonia

In Fig. 2, the peaks are more intense and sharper for the NaX + maximal  $\text{NH}_3$  spectrum (Fig. 2d) than in the other spectra. For

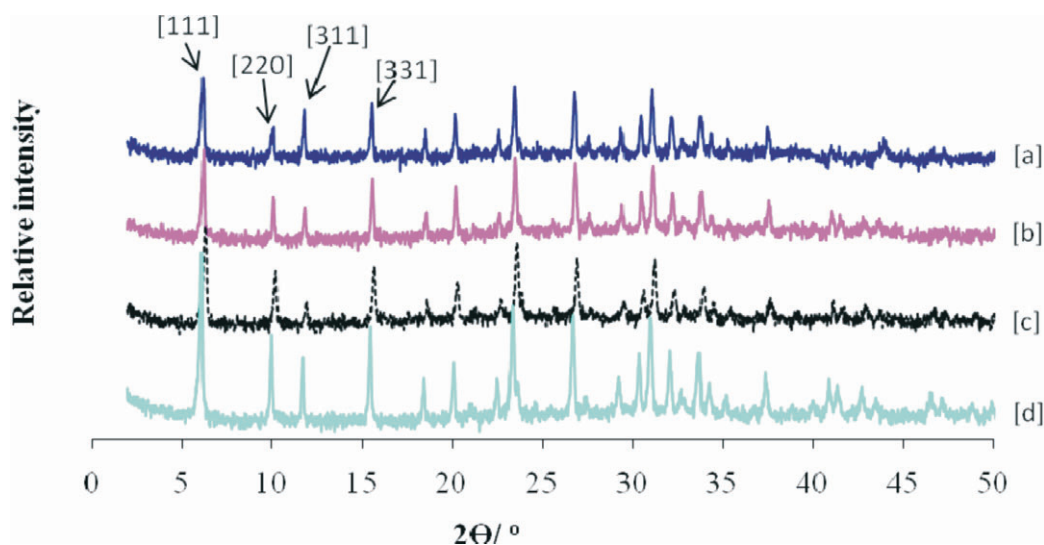


**Figure 2** The X-ray spectra of CuX with varying levels of ammonia exposure: (a), (b), (c) and (d) are for CuX + maximal  $\text{NH}_3$ , CuX +  $1/2 \text{ NH}_3/\text{Cu/UC}$ , CuX and NaX + maximal  $\text{NH}_3$  samples, respectively.

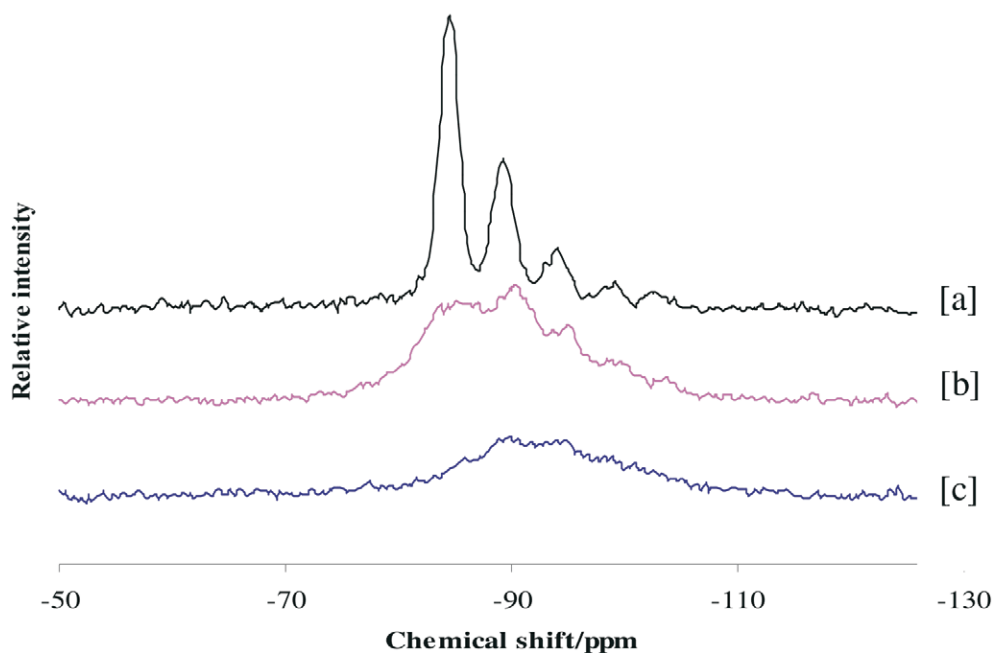


**Figure 3**  $^{29}\text{Si}$  MAS NMR spectra for (a) NaX, (b) 10 Cu/UC and (c) 24 Cu/UC.

the sample with  $\text{Cu}^{2+}$  exchange, a significant reduction in the relative intensity of the peak at  $11.9^\circ$  (311 indices) compared with that at  $10.12^\circ$  (220 indices) (Fig. 2c) belonging to NaX was recorded. However, upon the addition of ammonia into the samples (Figs. 2b and 2a), the peak at  $10.12^\circ$ , which in CuX had a higher intensity than the one at  $11.9^\circ$ , gradually decreased in intensity relative to the  $11.9^\circ$  peak.

### 3.3. $^{29}\text{Si}$ MAS NMR Study of CuX Before and After Exposure to Ammonia

All the  $^{29}\text{Si}$  NMR spectra in Fig. 3, especially for NaX (Fig. 3a), showed peaks at *ca.*  $\delta$  -85, -89, -95, -99 and -102 ppm. Figure 3 similarly shows that as the amount of Cu/UC increases, the signals get broader especially for the  $\delta$  -85 ppm peak.

Compared with the 24 Cu/UC (Fig. 3c), the copper (II) exchange at 10 Cu/UC (Fig. 3b) had an intermediate broadening effect on the intensity of the peak at  $\delta$  -85 ppm. Effects of exposure of the 10 and 24 Cu/UC to ammonia are presented in Fig. 4. The recovery in relative intensity for the 10 Cu/UC from the broadening effects of the paramagnetic  $\text{Cu}^{2+}$  ions, especially of the peak at  $\delta$  -85 ppm, is not complete (Fig. 4b), even after exposure to maximal ammonia.

However, the exposure of the 24 Cu/UC to maximal ammonia (Fig. 4a) is seen to restore the intensity and resolution of the peaks towards their pre-copper exchange levels even though the broadening is not completely lifted.

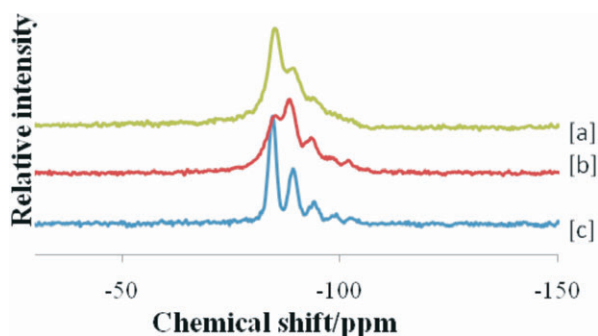


**Figure 4**  $^{29}\text{Si}$  MAS NMR spectra for (a) 24 Cu/UC + maximal ammonia, (b) 10 Cu/UC + maximal ammonia and (c) NaX + maximal ammonia.

### 3.4. Infrared Spectra of CuX Before and After Exposure to Ammonia

Upon exposure of CuX samples to ammonia, several changes were observed in their IR spectra; the  $896\text{ cm}^{-1}$  band which is pronounced in the CuX system completely disappears on addition of maximal ammonia (Fig. 5e). Other noticeable changes were for the Si-O-Al antisymmetric stretching edge at  $988\text{ cm}^{-1}$ , the S4R T-O-T symmetric stretching at  $756\text{ cm}^{-1}$ , the Si-O-Al symmetric stretching at  $685\text{ cm}^{-1}$ , and the S4R symmetric bending at  $455\text{ cm}^{-1}$  positions<sup>7</sup> shifting to 979, 752, 695 and  $460\text{ cm}^{-1}$  respectively (see Supplementary Material Figs. S3 and S4 for details). Figure 5 similarly shows a concomitant rise of the band at *ca.*  $1270\text{ cm}^{-1}$  and a corresponding disappearance of the shoulder at  $896\text{ cm}^{-1}$  with an increase in the amount of ammonia applied to the 24 Cu/UC. The data for 10 Cu/UC, which are not included in the text, showed a similar though weak band at *ca.*  $896\text{ cm}^{-1}$  which equally disappeared with addition of maximal ammonia (for details, see Supplementary Material, Figs. S3 and S4).

### 3.5. EPR of CuX Exposed to Ammonia

For low to moderate Cu/UC, the addition of ammonia broadened the hyperfine features in both the perpendicular and the parallel regions of each spectrum. Specifically for 1 Cu/UC, the two  $\text{Cu}^{2+}$  EPR species<sup>11</sup> associated with low Cu/UC were no longer resolvable after exposure to ammonia. However, the overall effects were statistically insignificant. For the 10 Cu/UC, some subtle changes were recorded for both the g and A spin Hamiltonian values after exposure to ammonia (see Supplementary material Table S1). The EPR spectrum (Fig. 6b) after exposure of the 24 Cu/UC to ammonia is sharper and more isotropic compared with that of the same sample when not exposed to ammonia. Figure 6b shows the loss of hyperfine features in the perpendicular region after exposure to ammonia. Due to the observed broadening, the  $g_{\text{iso}}$  value changes from *ca.* 2.16 to 2.11.

## 4. Analysis and Discussion

### 4.1. Effects of Exchange Levels on Framework Stability

From Fig. 1, the maximum copper (II) exchange level obtained was 38 Cu/UC. From our earlier work,<sup>11</sup> and both the DRS data in

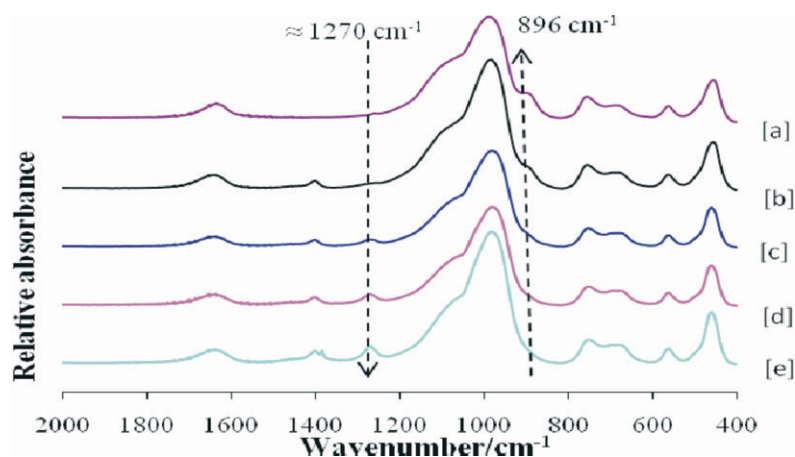


**Figure 5** Infrared spectra of the 24 Cu/UC exposed to varying amounts of ammonia in the range 2000–400  $\text{cm}^{-1}$ ; (a) 0, (b)  $\frac{1}{2}$ , (c) 1, (d) 2 and (e) 4  $\text{NH}_3/\text{Cu/UC}$ .

Fig. 1 and the XRD data in Fig. 2, we infer that up to the 24 Cu/UC level, the Cu (II) exchange procedure used here does not encourage Cu-Cu dimerization<sup>12</sup> to occur and that the crystallinity of the framework is also not yet compromised. Such a phenomenon, which implies that at 24 Cu/UC the zeolite structure is still intact, has also been noted by Hincapie *et al.*<sup>13</sup> However for exchange beyond 24 Cu/UC, possible Cu-Cu dimerization appeared, which in effect precludes the higher Cu/UC from use in this type of study. The Cu-Cu dimers had similarly been observed before.<sup>12</sup> Other workers have used higher exchange levels of 28 Cu/UC to study copper–zeolite interactions.<sup>14</sup>

#### 4.2. Effects of Ammonia on Site Location of $\text{Cu}^{2+}$

##### 4.2.1. At Low to Moderate ( $\leq 10$ Cu/UC) $\text{Cu}^{2+}$ Ion Exchange Levels

According to the structure of FAU-X,<sup>11</sup> ammonia may interact with  $\text{Cu}^{2+}$  ions only when the latter are either in site II or site III. The lack of significant changes in EPR spin Hamiltonian values after exposure to ammonia is consistent with insignificant interactions between ammonia and  $\text{Cu}^{2+}$  at 1 Cu/UC. However, for a zeolite with larger channels (CuMCM-41), Yu *et al.* report that ammonia, pyridine and water, among other adsorbates, bind  $\text{Cu}^{2+}$  even at such low Cu/UC levels.<sup>15</sup>

For the moderate Cu/UC ( $\approx 10$  Cu/UC) exchange levels, the  $^{29}\text{Si}$  NMR relative intensity of the  $\delta -85$  ppm signal shows that some reasonable fractions of  $\text{Cu}^{2+}$  ions are still magnetically in contact with the  $^{29}\text{Si}$ , forming Cu-O<sub>zeo</sub> bonds (Fig. 4) despite the exposure to maximal ammonia. In addition, the two IR bands for S6R Si-O-Al symmetric stretching at  $674 \text{ cm}^{-1}$  and S6R Si-O-Si symmetric stretching at  $696 \text{ cm}^{-1}$  in NaX<sup>7</sup> reappeared upon the

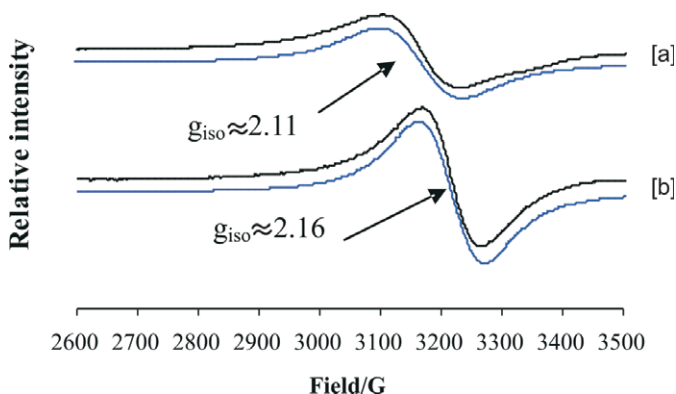
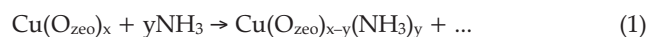


**Figure 6** The EPR spectra of (a) 24 Cu/UC and (b) 24 Cu/UC + maximal  $\text{NH}_3$ . The lower curve for each spectrum is the simulated spectrum.

exposure of the CuX to ammonia (see Supplementary Material Fig. S4 for details). The reappearance is consistent with  $\text{NH}_3$  reducing the effects of  $\text{Cu}^{2+}$  on the zeolite framework vibrational modes, mainly at S6R. Thus, the elimination of the IR SiO(-Cu)Al symmetric stretching band at  $896 \text{ cm}^{-1}$  (Fig. 5) is a manifestation of ammonia overcoming some Cu-O<sub>zeo</sub> interactions as depicted in Equation 1.



The nature of the  $\text{NH}_3$ - $\text{Cu}^{2+}$  interactions was then inferred from EPR data. According to models presented by Piesach and Blumberg<sup>16</sup> and Carl *et al.*,<sup>17</sup> and in consideration of the FAU topology,<sup>6</sup> the  $g_{\parallel} = 2.35$  and  $A_{\parallel}/g_e\beta_e = 170.0 \pm 8.4 \text{ G}$  ( $\approx 510 \text{ MHz}$ ) values imply a 2N2O (2 nitrogen atoms of the  $\text{NH}_3$  and 2 oxygen atoms of the zeolite) complexation for copper. The above deductions are depicted by the complex presented in the lower part of Fig. 7. This complex differs from the 3N3O species observed by Kieger *et al.* in CuX at higher temperatures.<sup>18</sup>

##### 4.2.2. At Higher Cu/UC Exchange Levels

Since the presence of more exchanged cations imbues host zeolites with more adsorbate holding capacity,<sup>19</sup> we expect more ammonia to be absorbed at 24 Cu/UC than at 10 Cu/UC. Consequently, a more effective redistribution of the  $\text{Cu}^{2+}$  ions within the framework at 24 Cu/UC is envisaged. Using these criteria, the reversal of the XRD relative intensities between the peaks at  $10.12$  and  $11.90^\circ$  (Fig. 2), corroborates the redistribution of copper from one site (possibly in the sodalite) to another (possibly in the supercage) under the influence of ammonia. Salama *et al.* had earlier observed a similar distribution in CuY.<sup>20</sup> The absence of any other changes in the NMR spectra (Fig. 3), except for the decrease in intensity witnessed for the  $\delta -85$  ppm peak, corroborates this redistribution. The above results show that, at 24 Cu/UC, ammonia is not moving the  $\text{Cu}^{2+}$  to any other new  $^{29}\text{Si}$  tetrahedral groups, but away from the influence of the whole zeolite framework. The framework-detached  $\text{Cu}^{2+}$  ion inevitably forms an isolated ligated complex in which the 'mobile' cation centre is not directly chemically attached to the zeolite framework. The broadened EPR spectrum in Fig. 6b attests to the existence the mobile  $\text{Cu}^{2+}$  ion centre.<sup>11</sup>

Upon deconvolution of the IR band at *ca.*  $1270 \text{ cm}^{-1}$  for samples in the entire Cu/UC range, two bands, one at  $1263 \text{ cm}^{-1}$  and the other at  $1272 \text{ cm}^{-1}$ , were obtained (see Supplementary Material Fig. S5 for details). From Fig. 7, the percentage area under the band at *ca.*  $1263 \text{ cm}^{-1}$  (prominent at  $\leq$  *ca.* 5 Cu/UC) decreases in relative intensity with increase in the amount of Cu/UC.



## Supplementary Material to:

C.O. Kowenje, D.C. Doetschman, J. Schulte, C.W. Kanyi, J. DeCoste, S.-W. Yang and B.R. Jones, *S. Afr. J. Chem.*, 2010, **63**, 6–10.

### A: The $^{29}\text{Si}$ MAS NMR Results

In Fig. S1, the increased broadening of the NMR peaks for the 10 Cu/UC sample can be seen not to recover completely even after exposure to maximal ammonia. The broadening effect is especially evident in the  $\delta$  -85 ppm peak at the low  $\delta$  edge of the spectrum. Thus at 10 Cu/UC, some Cu-O<sub>zeo</sub> interactions are not overcome by the presence of maximal ammonia.

In Fig. S2, the exposure of 24 Cu/UC to increasing amounts of ammonia is seen to decrease the broadening and improve the resolution of the peaks towards their appearances at pre-copper exchange levels. This effect is especially evident in the most intense  $\delta$  -85 ppm peak at the low  $\delta$  edge of the spectrum.

### B: The IR Results

The zeolite-metal ion symmetric stretching mode at 896  $\text{cm}^{-1}$  increases in intensity with an increase in the amount of  $\text{Cu}^{2+}$  applied per unit cell. The S4R T-O-T symmetric stretching

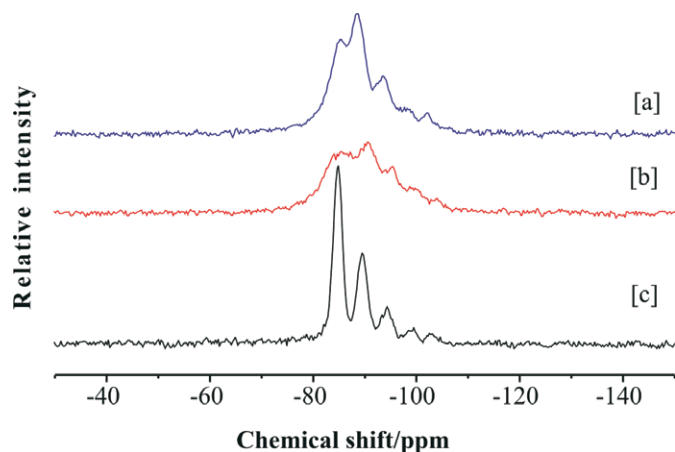


Figure S1  $^{29}\text{Si}$  MAS NMR for dehydrated (a) 10 Cu/UC + maximal  $\text{NH}_3$ , (b) 10 Cu/UC and (c) NaX + maximal  $\text{NH}_3$ .

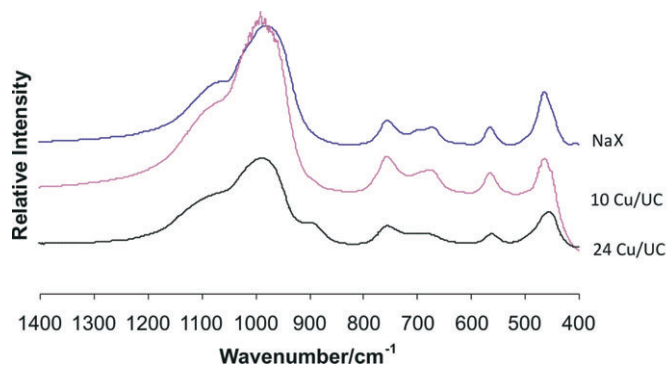


Figure S3 Infrared spectra in the 1400-400  $\text{cm}^{-1}$  region for various Cu/UC. (The NaX, 10 and 24 Cu/UC are offset by ca. 1, 2 and 3 absorbance units, respectively.)

vibration mode at 756  $\text{cm}^{-1}$  in dehydrated NaX did not shift, regardless of the amount of  $\text{Cu}^{2+}$  exchanged, while the D6R T-O-T symmetric stretching vibration at 566  $\text{cm}^{-1}$  shifted to a constant position of 562  $\text{cm}^{-1}$  for all the samples. Notably, the intensity of the 6R ring vibration mode at 407  $\text{cm}^{-1}$  decreased as the amount of  $\text{Cu}^{2+}$  exchange increased.<sup>1-3</sup>

In Fig. S4, several IR bands are shifted upon exposure of the CuX to ammonia, the S4R, the T-O-T symmetric stretching band at 756  $\text{cm}^{-1}$ , the Si-O-Al symmetric stretching band at 685  $\text{cm}^{-1}$  and the S4R symmetric bending band at 455  $\text{cm}^{-1}$  (refs 1-3) moving to 979, 752, 695 and 460  $\text{cm}^{-1}$  respectively. The D6R was minimally shifted from 561 to 563  $\text{cm}^{-1}$ , a shift that is considered to be within the experimental error.

The deconvolution of the band at approximately 1270  $\text{cm}^{-1}$  reveals the two species presented in Fig. 7 of the main text. From Fig. S5, as the concentration of the Cu/UC increases, the other species at ca. 1272  $\text{cm}^{-1}$  becomes more dominant.

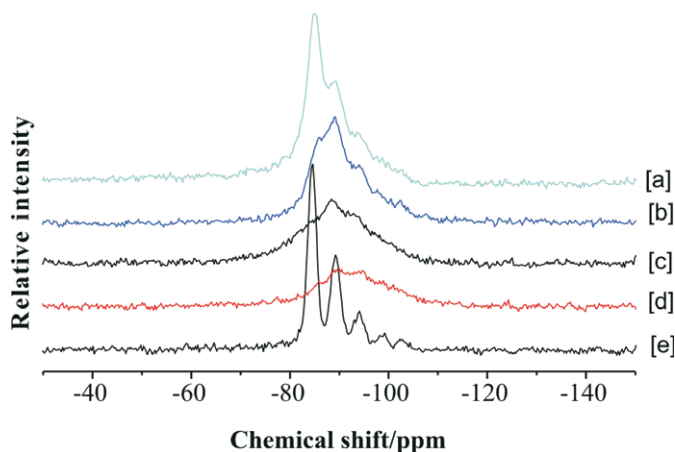


Figure S2  $^{29}\text{Si}$  MAS NMR for dehydrated (a) CuX + maximal  $\text{NH}_3$ , (b) CuX + 3  $\text{NH}_3$ , (c) CuX + 1  $\text{NH}_3$ , (d) CuX and (e) NaX + maximal  $\text{NH}_3$ .

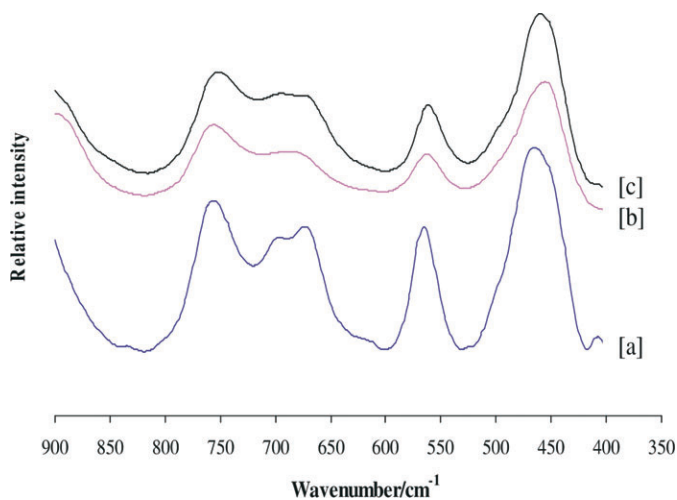
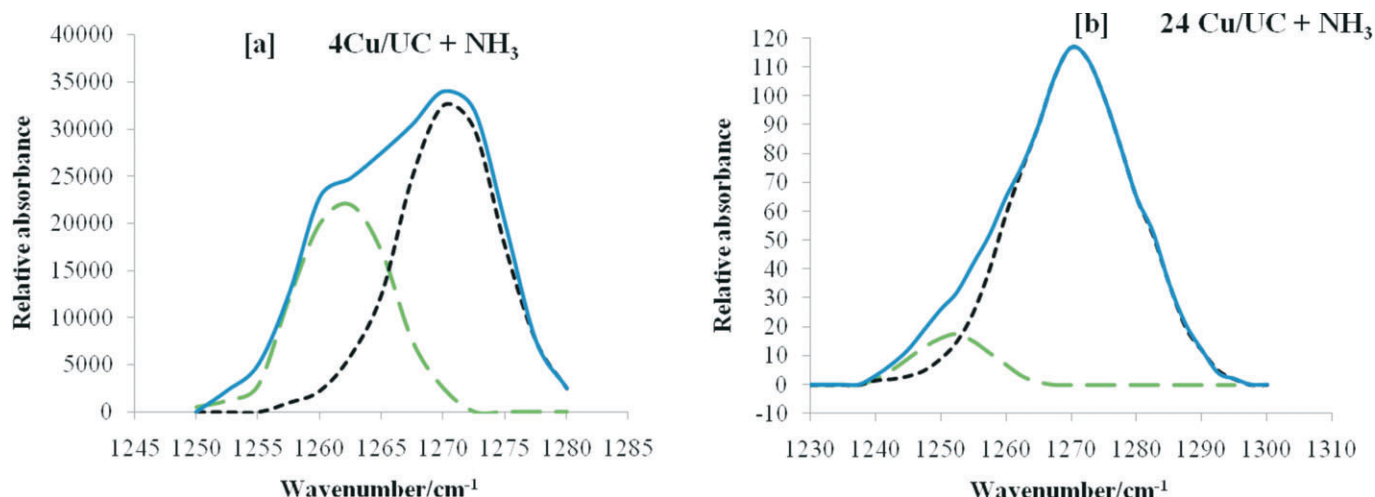


Figure S4 Effects of exposure to ammonia in the ring IR band regions of the zeolite: (a) for NaX, (b) for 24 Cu/UC and (c) for 24 Cu/UC + ammonia.



**Figure S5** The deconvolved  $ca. 1270\text{ cm}^{-1}$  band for various Cu/UC exposed to maximal ammonia. The fitted spectrum on the left occurs at  $ca. 1263\text{ cm}^{-1}$  while that on the right occurs at  $ca. 1272\text{ cm}^{-1}$ . The graphs are for (a) 4 and (b) 24 Cu/UC samples. To bring them to scale, the absorbances of (a) and (b) were multiplied by  $7 \times 10^4$  and 60, respectively.

### C: The EPR Results

From Table S1, the changes brought about by the exposure to maximal ammonia were not significant for the case of 1 Cu/UC. However, some measurable changes were recorded for 10 Cu/UC.

### References

- 1 C.S. Blackwell, *J. Phys. Chem.* 1979, **83**, 3257–3261.
- 2 J. Dwyer and R. V. Parish, *Inorg. Chim. Acta*, 1983, **75**, 229–234.
- 3 W. Mazgawa, *J. Mol. Structure*, 2001, **596**, 129–137.

**Table S1** Spin Hamiltonians for 1 and 10 Cu/UC with and without ammonia. For 1 Cu/UC,  $A_x = A_y \approx 0$ ,  $A_z = A_{\parallel}$ . The asterisks indicate values for which minimization could not be attained.

Sample	g value		Hyperfine splitting (A)/G		Line width (L)/G	
	$g_{\parallel}$	$g_{\perp}$	$A_{\parallel}$	$A_{\perp}$	$L_{\parallel}$	$L_{\perp}$
1Cu/UC; species (I)	2.363 (0.001)	2.051 (0.001)	127.0 (3.8)		55.0 (2.1)	45.5 (2.0)
1Cu/UC; species (II)	2.337 (0.002)	2.071 (0.006)	148.3 (4.8)		60.0 (3.0)	42.0 (2.5)
1 Cu/UC + ammonia	2.347 (0.011)	2.047 (0.002)	170.0 (15.0)		60.0 (10.0)	45.0 (4.1)
10 Cu/UC	2.320 (0.005)	2.066 (0.002)	140.0 (10.0)	93.0 (8.9)	55.5 (4.5)	47.0 (2.8)
10 Cu/UC + ammonia	2.35 (0.009)	2.080 (0.005)*	170.0 (8.4)*	99.7 (6.3)	60.2 (10.4)	49.8 (5.1)*